Geomechanics and Engineering, *Vol. 30, No. 6 (2022) 551-564*
https://doi.org/10.12989/gae.2022.30.6.551

Development of a new explicit soft computing model to predict the blast-induced ground vibration

Saif Alzabeebee[1], Mehdi Jamei[2], Mahdi Hasanipanah[3], Hassan Bakhshandeh Amnieh[4], Masoud Karbasi[5] and Suraparb Keawsawasvong*[6]

[1]*Department of Roads and Transport Engineering, University of Al-Qadisiyah, Iraq*
[2]*Engineering Faculty, Shohadaye Hoveizeh Campus of Technology, Shahid Chamran University of Ahvaz, Dashte Azadegan, Khuzestan, Iran*
[3]*Department of Mining Engineering, University of Kashan, Kashan, Iran*
[4]*School of Mining, College of Engineering, University of Tehran, Tehran 11155-4563, Iran*
[5]*Water Engineering Department, Faculty of Agriculture, University of Zanjan, Zanjan, Iran*
[6]*Department of Civil Engineering, Thammasat School of Engineering, Thammasat University, Pathumthani, 12120, Thailand*

(*Received April 27, 2022, Revised August 31, 2022, Accepted September 8, 2022*)

Abstract. Fragmenting the rock mass is considered as the most important work in open-pit mines. Ground vibration is the most hazardous issue of blasting which can cause critical damage to the surrounding structures. This paper focuses on developing an explicit model to predict the ground vibration through an multi objective evolutionary polynomial regression (MOGA-EPR). To this end, a database including 79 sets of data related to a quarry site in Malaysia were used. In addition, a gene expression programming (GEP) model and several empirical equations were employed to predict ground vibration, and their performances were then compared with the MOGA-EPR model using the mean absolute error (MAE), root mean square error ($RMSE$), mean (μ), standard deviation of the mean (σ), coefficient of determination (R^2) and $a20-index$. Comparing the results, it was found that the MOGA-EPR model predicted the ground vibration more precisely than the GEP model and the empirical equations, where the MOGA-EPR scored lower MAE and $RMSE$, μ and σ closer to the optimum value, and higher R^2 and $a20-index$. Accordingly, the proposed MOGA-EPR model can be introduced as a useful method to predict ground vibration and has the capacity to be generalized to predict other blasting effects.

Keywords: blasting, ground vibration, multi objective genetic algorithm evolutionary polynomial regression, prediction models

1. Introduction

The use of explosives material is considered as a well-known economical method to fragment and displace rock mass in surface mines. However, it produces several environmental issues such as flyrock and ground vibration (Hajihassani *et al.* 2015, Hasanipanah *et al.* 2015, Koopialipoor *et al.* 2019, Hasanipanah and Amnieh 2020a). The ground vibration is the most hazardous issue of blasting which results in various damages for the surrounding structures (Ghasemi *et al.* 2013, Saadat *et al.* 2014, Hajihassani *et al.* 2015, Abbas and Asheghi 2018, Nguyen *et al.* 2020). Hence, it needs to be predicted with a high degree of accuracy to reduce the potential risk of damage. One of the most important descriptors to determine the ground vibration is the peak particle velocity (PPV) and has been used in many studies (Khandelwal *et al.* 2011, Nguyen *et al.* 2020). By reviewing the previous studies in the field of blasting-vibration, it can be found that the PPV is related to some controllable and uncontrollable parameters (Hasanipanah *et al.* 2017, Armaghani *et al.* 2020). The controllable parameters mean the blast design parameter, and engineers can control to some extend these parameters in the site, such as burden, spacing and weight of charge used in the blasting. On the other hands, other parameters such as properties of rock mass, have considerable effect on the PPV and considered as uncontrollable parameters. Among the controllable and uncontrollable parameters, the distance between the blasting point and the nearest structure is very important parameter especially for safety issues. Hence, due to the importance of accurate prediction of the PPV, there has been attempt in the literature to develop empirical equations to predict it to quantify the vibration associate with the blasting (Duvall and Petkof 1959, Davies *et al.* 1964, Langefors and Kihlstrom 1963, Ambraseys and Hendron 1968). These empirical equations are formulated considering only two parameters, these parameters are the maximum charge weight per blasting delay (W) and the distance of the PPV measurement (D). Other blast design parameters also influence the intensity of PPV, however, these have not been considered in the aforementioned references due to the complexity of the interrelationship between the parameters (variables). To resolve this problem, new machine learning methods have been employed in the literature to predict the PPV using more than two variables (e.g., Armaghani *et al.* 2020, Nguyen *et al.* 2020a,b, Rajabi and Vafaee 2020, Jelušič *et al.* 2021). Monjezi *et al.* (2013) developed an artificial neural network (ANN) model and

*Corresponding author, Ph.D.
E-mail: ksurapar@engr.tu.ac.th

ISSN: 2005-307X (Print), 2092-6219 (Online)

Table 1 Some recently published papers in the field of blast induced PPV

Models	Performance	References
Fs-RF	R^2=0.90	Zhou *et al.* (2020)
HKM-ANN	R^2=0.98	Nguyen *et al.* (2020)
RVR-GWO	R^2=0.92	Fattahi and Hasanipanah (2021)
CSO-ANN	R^2=0.987	Bui *et al.* (2021)
MARS	R^2=0.71	Arthur *et al.* (2020)
MARS-PSO-MLP	R^2=0.90	Nguyen *et al.* (2021)
PSO-CRANFIS	R^2=0.99	Zhu *et al.* (2021)
HHO-RF	R^2=0.94	Yu *et al.* (2020)
SCA-ANN	R^2=0.999	Lawal *et al.* (2021a)
WOA-XGBoost	R^2=0.98	Qiu *et al.* (2021)
MFO-ANN	R^2=0.9577	Lawal *et al.* (2021b)

R^2: Coefficient of determination, Fs: Feature selection, RF: Random forest, HKM: Hierarchical k-means clustering, ANN: artificial neural network, RVR: Relevance vector regression, GWO: Grey wolf optimization, CSO: Cuckoo search optimization, MARS: Multivariate Adaptive Regression Splines, PSO: Particle swarm optimization, MLP: Multiple layers perceptron neural network, CRANFIS: chaos recurrent ANFIS, HHO: Harris hawks optimization, SCA: sine cosine algorithm, XGBoost: extreme gradient boosting, MFO: moth-flame optimization algorithm.

empirical equation to predict the PPV. The study involved using a database gathered from the Shur river dam region in Iran. Comparison between the ANN and the empirical equations revealed the acceptability of the ANN in this field. Hasanipanah *et al.* (2017) investigated the use of classification and regression tree (CART) method in predicting the PPV. In addition, classical regression analysis was also applied. According to their results, the CART method was found to be better than the classical regression analysis to predict the PPV. In another research, an optimized XGBoost method was proposed to predict the PPV by Zhang *et al.* (2019). In this regard, a common optimization algorithm, namely particle swarm optimization (PSO) was employed to optimize XGBoost method. The results showed that the XGBoost-PSO method predicted the PPV with higher accuracy compared to other empirical equations. A practical scheme of quantile regression neural network method in combination with fuzzy C-means clustering (QRNN-FCM) was proposed by Bui *et al.* (2020) to predict the PPV. Other machine learning methods, namely the ANN and random forest were also used in their study. From their results, the QRNN-FCM method showed better accuracy in the prediction of the PPV compared to other machine learning methods. Furthermore, other researchers used hybrid models to predict the PPV. Nguyen *et al.* (2020) combined the ANN and k-means clustering algorithm (HKM) methods. Fang *et al.* (2019a) combined the M5Rules and imperialist competitive algorithm (ICA). Also, Ding *et al.* (2019) combined the XGBoost and ICA. In their studies, some other machine learning methods were also used for comparison aims. They confirmed the acceptability and reliability of the proposed hybrid models in this field. In other studies, PSO, genetic and firefly algorithms were applied to optimize the support vector regression (SVR) (Chen *et al.* 2021). Their results indicated that the optimization algorithms successfully improved the performance of the SVR and recommended to use these methods in the field of PPV prediction. Table 1 show other recently published papers on the prediction of the PPV using soft computing techniques.

Table 2 statistics of the database used in this study

Descriptive statistics	Parameters					
	W (kg)	B/S	SL (m)	Vp (m/s)	D (m)	PPV
Mean	421.95	0.820	5.32	3728.58	311.32	13.02
St. Error	17.97	0.002	0.22	56.06	10.29	0.70
Kurtosis	-1.24	-0.90	-1.09	-1.31	0.36	0.24
Skewness	-0.34	0.310	-0.38	-0.11	-1.09	0.73
Min	133.59	0.780	1.50	2876.00	100.00	2.83
Max	642.51	0.890	8.00	4506.00	440.00	30.06

It is clear based on this brief review that there have been many studies on the use of soft computing to predict the PPV, however, all of these studies did not propose an explicit formulation based on soft computing to facilitate robust prediction to ensure accurate prediction of the PPV. Thus, the objective of this paper is to develop robust and accurate explicit models to compute the PPV using advanced soft computing techniques. For this purpose, a multi objective genetic algorithm evolutionary polynomial regression (MOGA-EPR) analysis has been employed to develop the predictive model. In addition, the accuracy of the new model has been compared with the gene expression programming (GEP) and several empirical equations to illustrate the accuracy of the developed model.

It is worthy to state that the main reason to use the MOGA-EPR and GEP techniques in this paper is because these two techniques provide explicit mathematical models that can be easily interpreted and used in future studies (Alzabeebee and Chapman 2020).

2. Field investigation

In the present study, a granite quarry, namely the Harapan Ramai, located in Malaysia was investigated and the required data were carefully measured. To displace the rock mass, drilling and blasting methods was performed in the quarry, hence, their undesirable effects were inevitable. In the site, the holes were drilled with a diameter of 150 mm, and then the drilled holes were charged by the dynamite and ANFO as the main initiation and explosive materials, respectively. As stated earlier, some blast design parameters as well as properties of rock remarkably influence the PPV. In this study, the the maximum charge weight per blasting delay (W), the distance of the PPV measurement (D), burden to spacing ratio (B/S), stemming length (SL) and P-wave velocity (Vp) were considered as the input parameters. The values of W, B/S and SL were measured through blasting pattern. To measure the value of Vp, the samples were analyzed in the laboratory through the recommended process by the International Society for Rock Mechanics (ISRM). In addition, the value of D was measured by using GPS (distance between the blasting point and installed seismograph). The VibraZEB

seismograph was installed to the PPV values carefully in different locations. The values of aforementioned parameters related to 79 blasting events were used in this study. A statistical view of the obtained results (used dataset) is given in Table 2.

3. Theoretical overview of the employed soft computing techniques

As stated in the introduction, the MOGA-EPR and GEP algorithm have been employed in this study to develop models to predict the PPV. A brief review of these models is explained in the next subsections.

3.1 MOGA-EPR

The multi objective genetic algorithm evolutionary polynomial regression analysis (MOGA-EPR) is a hybrid regression method combines the flexibility of the regression analysis with the genetic programming to provide a symbolic model. This method has been developed by Giustolisi and Savic (2009) based on the older version of the method which has also been developed by the same authors (Giustolisi and Savic 2006).

In the MOGA-EPR, the genetic algorithm is employed in the first step to search for the best combination of the exponents of the developed model. The second step focuses on the determination of the model constants utilizing the least square method which has the ability to solve overdetermined systems (i.e., systems with number of equations more than the number of constants). On the other hand, a multi-objective algorithm based on Pareto dominance criterion is used to control the fitness of the model in one objective and control the complexity of the developed model utilizing at least on more objective (Alzabeebee 2022a). Finally, it is worthy to add that the MOGA-EPR searches for all of the candidate models (i.e., models with different number of terms) simultaneously and ranked these models according to the number of terms and the accuracy achieved (Giustolisi and Savic 2009).

The strength of the MOGA-EPR is that it provides relatively simple model compared with other soft computing techniques (Alzabeebee 2022b, Alzabeebee and Chapman 2020). In addition, many previous studies proved the efficiency of the MOGA-EPR in developing simple and robust models for many applications in civil engineering (Alzabeebee *et al.* 2022b, Alzabeebee 2019, 2020, 2022, Shams *et al.* 2020, Wang *et al.* 2020, Zuhaira *et al.* 2021). The general formulation of the MOGA-EPR is shown in Eq. (1) (Giustolisi and Savic 2006, 2009).

$$Y = \sum_{j=1}^{m} a_j . z_j + a_o \tag{1}$$

Where, Y is the output symbolic model, which is used to predict the dependent variable, a_j is the constant for each z_j term, a_o is the bias of the symbolic model, m is the number of the suggested terms for the symbolic model, and z_j is the transformed variable. It is worthy to state that z_j (for example) is obtained using Eq. (2). However, Eq. (2) changes based on the proposed structure for the polynomial model, which will be discussed further in Eq. (3).

$$z_j = x_1^{ES(j,1).} \dots x_i^{ES(j,1).} \dots x_k^{ES(j,1)} \tag{2}$$

Where, x_i is the ith input variable, k is the number of the input variables used in the model development, $\mathbf{ES}_{mxK}$ is the matrix of the exponents. The exponents range is specified by the user, however, the distribution of the exponents is decided by GA via evolutionary process.

In addition, Y can be structured using different polynomial expressions as shown in Eq. (3) (Giustolisi and Savic 2009).

$$\begin{gathered}
Y = a_0 + \sum_{j=1}^{m} a_j (X_1)^{ES(j,1).} \dots (X_k)^{ES(j,k)} f((X_1)^{ES(j,k+1)}) \dots f((X_k)^{ES(j,2k)}) \\
Y = a_0 + \sum_{j=1}^{m} a_j f((X_1)^{ES(j,1).} \dots (X_k)^{ES(j,k)}) \\
Y = a_0 + \sum_{j=1}^{m} a_j (X_1)^{ES(j,1).} \dots (X_k)^{ES(j,k)} f((X_1)^{ES(j,k+1).} \dots (X_k)^{ES(j,2k)}) \\
Y = \log\left(a_0 + \sum_{j=1}^{m} a_j (X_1)^{ES(j,1).} \dots (X_k)^{ES(j,k)}\right) \\
Y = \log\left(a_0 + \sum_{j=1}^{m} a_j (X_1)^{ES(j,1).} \dots (X_k)^{ES(j,k)}\right) \\
Y = \sin\left(a_0 + \sum_{j=1}^{m} a_j (X_1)^{ES(j,1).} \dots (X_k)^{ES(j,k)}\right) \\
Y = \tan\left(a_0 + \sum_{j=1}^{m} a_j (X_1)^{ES(j,1).} \dots (X_k)^{ES(j,k)}\right)
\end{gathered} \tag{3}$$

3.2 GEP

The GEP is a convenient way to model nonlinear and complex processes (Aytek and Kişi 2008, Faradonbeh *et al.* 2016). In the present study, GEP, which is an extended form of genetic programming (GP) (Ferreira 2001), is used to predict the PPV. This type of algorithm encodes individuals in the form of linear chromosomes which have fixed length and can be expressed in the form of tree structures (Ferreira 2002). Genetic operators such as mutation and recombination can be used considering linear structure of chromosomes. These operators can produce correct and valid structures for solution. In the present study the GeneXproTools software has been used to perform the GEP analysis (Gandomi *et al.* 2015). The first step in this method is to generate the initial population of solutions using a series of functions and terminals. A set of functions, usually including basic arithmetic functions {+, -, ×, /}, trigonometric, logarithmic, polynomial functions or any other mathematical non-linear functions {√, x^2, exp, tan, log, cos sin, ln, ...} which are suitable for model interpretation (Gholampour *et al.* 2017). The set of terminals consists of constant values and independent problem variables. Chromosomes are then represented as tree expressions. In the next step, the efficiency or compatibility of each member of the chromosome population should be evaluated using the fitting function. The fitting function used in this research is defined as follows (Koza 1992)

$$f_i = \sum_{j=1}^{n} \left(R - \left| \frac{P_{ij} - T_j}{T_j} \right| \times 100 \right) \tag{4}$$

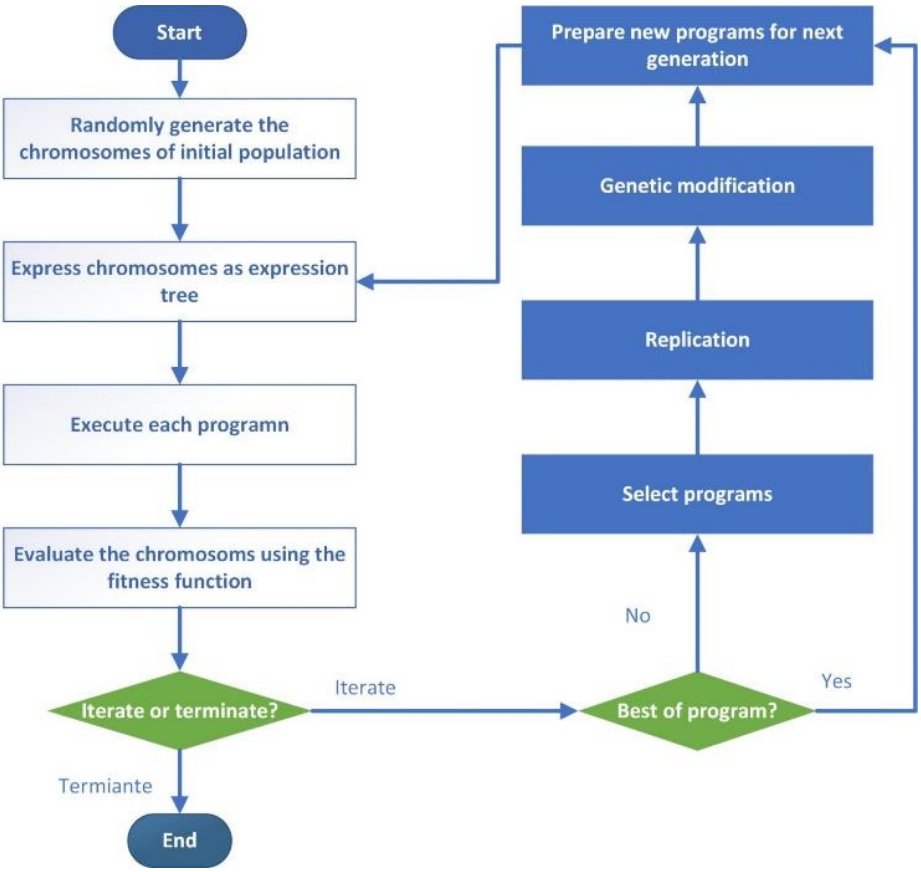

Fig. 1 Flowchart of GEP (Faradonbeh *et al*. 2016)

In the above equation, P_{ij} is the value predicted by i th chromosome for the fitness case j, R is the range of selection, and T_j is the target value for the fitness case j. Thus, with the help of the fit function and maintaining the superior answers and eliminating the weaker answers, we get closer to the desired answer. Therefore, the relationship between dependent and independent variables is not constant and is constantly changing. In general, the step-by-step process of the GEP model is as follows (Gholampour *et al.* 2017):

1. The process begins with the random production of chromosomes from the initial population.
2. Chromosomes are expressed as tree expressions.
3. The degree of desirability of each potential solution of the problem (chromosome) and its degree of compatibility is evaluated.
4. If the desired conditions are achieved, the program is stopped, and the existing population shows the desired answer.
5. The best people from the present population are kept.
6. The rest of the population is selected based on their performance.
7. Corrections and improvements remade on the selected population, as a result, children with new characteristics are produced.
8. New offspring go through the same developmental process in a cycle, and this process is repeated for a definite number of generations to find a suitable solution.

The flowchart of GEP is illustrated in Fig. 1.

4. Available empirical equations to predict the PPV

Many researchers have attempted to present empirical equations to predict the PPV. These empirical equations depend merely on two parameters, W and D. In this study, four common empirical equations were used for comparison purposes. These equations are Duvall and Petkof (1959), Ambraseys-Hendron (1968), Langefors-Kihlstrom (1963) and Davies *et al.* (1964). The mathematical formulation of these equations explained as follows:

Duvall and Petkof (1959)

$$PPV = K \times \left(\frac{D}{W^{1/2}}\right)^n \quad (5)$$

Ambraseys-Hendron (1968)

$$PPV = K \times \left(\frac{D}{W^{1/3}}\right)^n \quad (6)$$

Langefors-Kihlstrom (1963)

$$PPV = K \times \left(\frac{W^{1/2}}{D^{3/4}}\right)^n \quad (7)$$

Davies *et al.* (1964)

$$PPV = K \times D^a \times W^b \quad (8)$$

Where, K, n, a and b are site constants and can be calculated using SPSS or Excel programs.

5. Statistical indicators to check the models

To check the accuracy of the predictive models, several statistical indicators are employed based on previous studies on the topic (Zhou *et al.* 2015, 2016, 2017, 2019, Hasanipanah *et al.* 2020a, b, Alkroosh *et al*., 2020, Zhang *et al.* 2020, 2021a, b, Hasanipanah and Amnieh 2020b, Huang *et al.* 2020, 2021, Alzabeebee *et al*. 2022b, Armaghani *et al*. 2021, Bai *et al*. 2021, Kamran *et al*. 2022, Kwak and Ko 2022, Luat *et al*. 2021a, b, Sasmal and Behera 2022, Zhang *et al*. 2022). These indicators are:

Mean absolute error (MAE)

$$MAE = \frac{1}{n}\sum_1^n \left|PPV_m - PPV_p\right| \quad (9)$$

Root mean square error ($RMSE$)

$$RMSE = \sqrt{\frac{1}{n}\sum_1^n (PPV_m - PPV_p)^2} \quad (10)$$

Mean (μ)

$$\mu = \frac{1}{n}\sum_1^n \left(\frac{PPV_p}{PPV_m}\right) \quad (11)$$

Standard deviation (σ)

$$\sigma = \sqrt{\frac{\sum_1^n \left(\frac{PPV_p}{PPV_m} - \mu\right)^2}{n-1}} \quad (12)$$

Coefficient of determination (R^2)

$$R^2 = \left(\frac{\sum_{i=1}^n (PPV_p - PPV_{p_{average}})(PPV_m - PPV_{m_{average}})}{\sqrt{\sum_{i=1}^n (PPV_p - PPV_{p_{average}})^2 \sum_{i=1}^n (PPV_m - PPV_{m_{average}})^2}}\right)^2 \quad (13)$$

Percentage of prediction within error of ±20%

$$a20 - index = \frac{mp20}{n} \quad (14)$$

In the above equations, PPV_m and PPV_p are the measured and predicted PPV values. The n is the number of data, and $mp20$ is the number of predictions within error range of $\pm 20\%$. It is worth mentioning that $a20 - index$ declares the amount of the data that satisfies predicted values with a deviation ±20% compared to measured values (Alzabeebee and Chapman 2020). For a perfect predictive model, the value of $a20 - index$ is expected to be equal to 1. Thus, the use of $a20 - index$ is deemed necessary as it explicitly shows the percentage of predictions within acceptable error of prediction and thus, explicitly illustrate the best model in terms of accuracy.

6. Application results and analysis

The results of the empirical equations, development of the MOGA-EPR and GEP models are presented in this section. It is worth stating that for the development of the GEP and MOGA-EPR models, the database has been divided into training and testing sets where 80% of the data has been utilized to train the models using the GEP and MOGA-EPR, while the rest of the data has been used to test the performance of the model. This step has been undertaken to ensure that the proposed model has the ability to predict results that did not influence the model training. This approach is not uncommon in soft computing of the relationship between the dependent and independent variables. Hence, the statistical analysis for the empirical equations has been done for training and testing datasets separately to guarantee consistent comparisons with the empirical equations.

It is necessary to add that the data is divided into training and testing using random shuffle function available in excel combined with statistical analysis to ensure that the testing data are within the range of the training data to avoid extrapolation in estimation (Alzabeebee 2022b). Tables 3 and 4 present the statistics of the data used for training and testing, respectively.

Table 3 Statistics of the training data

Statistic indicator	W	B/S	SL	Vp (m/s)	D (m)	PPV (mm/s)
Min	133.59	0.79	1.50	2876.00	100.00	2.83
Max	642.52	0.89	8.00	4506.00	440.00	30.06
Average	420.97	0.83	5.32	3714.06	312.81	12.85

Table 4 Statistics of the testing data

Statistic indicator	W	B/S	SL	Vp (m/s)	D (m)	PPV (mm/s)
Min	133.59	0.79	1.50	3034.00	100.00	3.36
Max	642.52	0.87	8.00	4344.00	420.00	26.76
Average	425.83	0.82	5.33	3785.75	305.50	13.71

7. Statistical assessment of the available empirical equations

As stated earlier, the values of site constants in the empirical equations can be calculated through the Excel program. Based on the calculations, the used empirical equations were updated as follows

$$PPV = 187.26 \times \left(\frac{D}{W^{1/2}}\right)^{-1.31} \quad (15)$$

$$PPV = 402.99 \times \left(\frac{D}{W^{1/3}}\right)^{-0.94} \quad (16)$$

$$PPV = 71.84 \times \left(\frac{W^{1/2}}{D^{3/4}}\right)^{1.49} \quad (17)$$

$$PPV = 178.79 \times D^{-1.12} \times W^{0.52} \quad (18)$$

where, W, D and PPV are in terms of kg, m and mm/s, respectively. The performance of above empirical equations is illustrated through Fig. 2 and Tables 5 and 6. In addition, the perfect fit line (i.e., the line of no error) and the ±20% error range have also been presented in Figure 2 for illustration purposes. As shown in these figures, the R^2 values obtained from empirical equations were around 0.8 for training and testing datasets. This indicates that the performance of empirical equations is in an average range. In addition, by comparing the statistical performance of the equations using the measures reported in Tables 5 and 6, it is clear that the equations of Ambraseys-Hendron (1968)

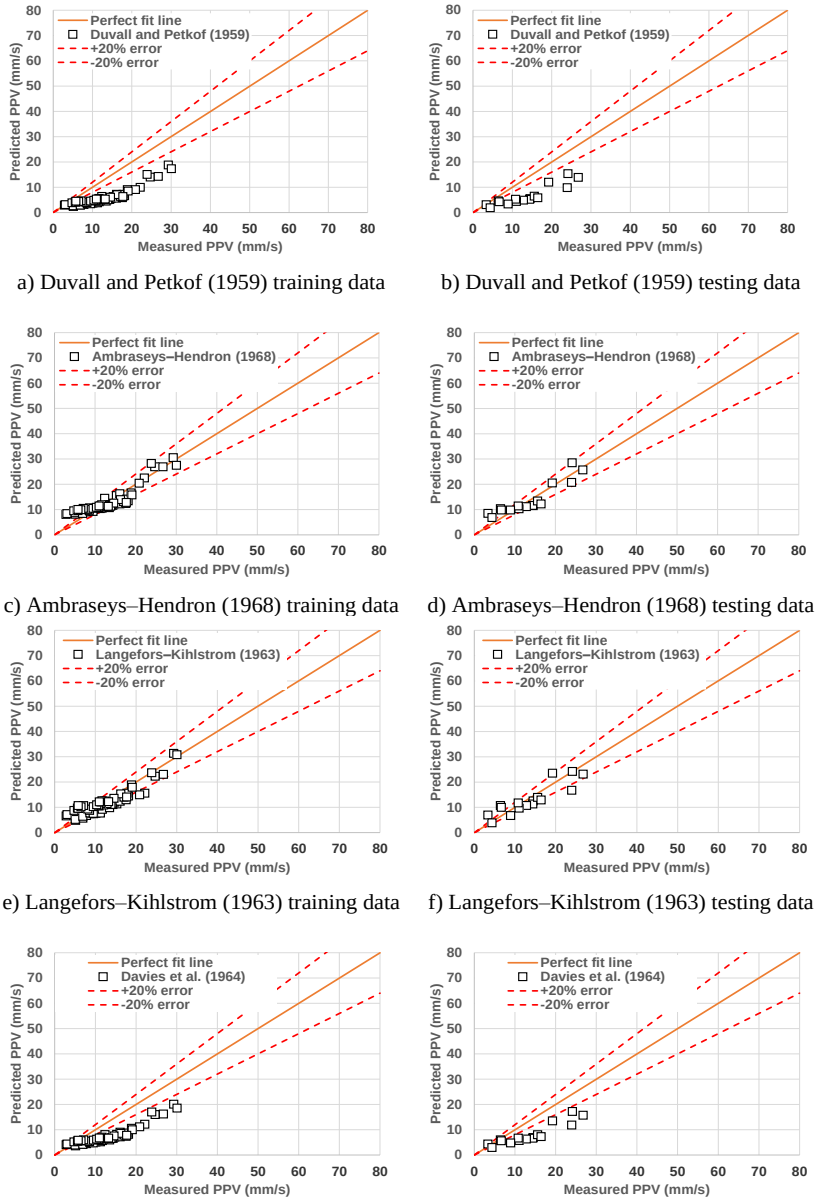

a) Duvall and Petkof (1959) training data b) Duvall and Petkof (1959) testing data

c) Ambraseys–Hendron (1968) training data d) Ambraseys–Hendron (1968) testing data

e) Langefors–Kihlstrom (1963) training data f) Langefors–Kihlstrom (1963) testing data

g) Davies et al. (1964) training data h) Davies et al. (1964) testing data

Fig. 2 Relationship between measured and predicted results using the empirical equations

Table 5 Statistical performance indicators of the available empirical equations for training data

Model	MAE	$RMSE$	μ	σ	$a20-index$	R^2
Duvall and Petkof (1959)	6.93	7.66	0.48	0.15	0.05	0.82
Ambraseys-Hendron (1968)	2.09	2.61	1.12	0.42	0.67	0.81
Langefors-Kihlstrom (1963)	2.18	2.67	1.01	0.36	0.63	0.83
Davies *et al.* (1964)	5.55	6.30	0.62	0.21	0.10	0.84

Table 6 Statistical performance indicators of the available empirical equations for testing data

Model	MAE	$RMSE$	μ	σ	$a20-index$	R^2
Duvall and Petkof (1959)	7.07	8.04	0.51	0.16	0.06	0.81
Ambraseys-Hendron (1968)	2.54	2.89	1.16	0.46	0.63	0.83
Langefors-Kihlstrom (1963)	2.71	3.21	1.05	0.38	0.50	0.79
Davies *et al.* (1964)	5.71	6.67	0.65	0.23	0.13	0.83

and Langefors-Kihlstrom (1963) achieved better prediction accuracy compared with other equations where these equations scored the lowest MAE and $RMSE$, the highest μ (which is close to 1.0) and the highest $a20-index$ (which is equal to 0.67 and 0.63, respectively for training dataset and 0.63 and 0.50, respectively for testing dataset).

8. Development of the GEP model

The model is provided based on five input variables including W, D, B/S, SL and Vp. Table 7 reports the main setting parameters of the GEP model which is developed by using simple mathematical operators (+, −, ×, and /) to be

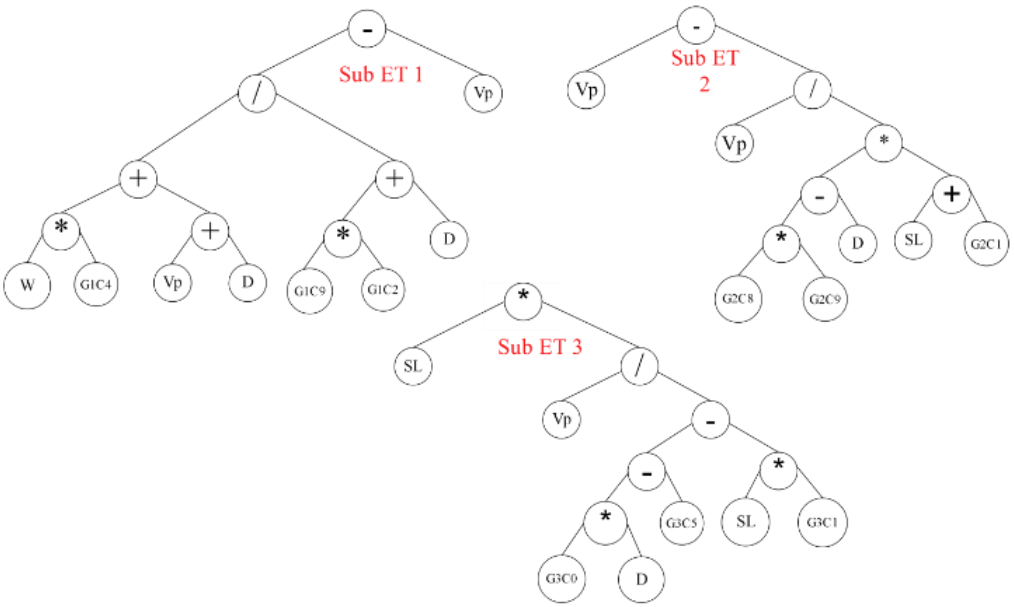

Fig. 3 The expression tree obtained using GEP model to predict the PPV

Table 7 The main setting parameters and adjustments of GEP model

GEP parameter	Setting of parameters
Number of chromosomes	30
Head size	6
Number of genes	5
Function set	+, −, ×, and /
Fitness function	RMSE
Mutation rate	0.00138
Inversion rate	0.00346
Gene transposition rate	0.00227
Random chromosomes	0.0026
Gene recombination rate	0.00227

easily used for researchers. The extracted relationship of the model and the tree-based model of the GEP model are shown in Table 8 and Fig. 3, respectively. The performance of GEP model is illustrated through Figs. 4 and 5 for both testing and training data. As shown in these figures, the R^2 value obtained from the model is equal to 0.93 for training data and 0.89 for testing data. This indicates that the performance of GEP is in a good range and better than empirical equations. Also, and as shown in Fig. 5, the GEP model scored better in terms of the MAE, $RMSE$, μ, σ, and $a20-index$ compared with the aforementioned empirical equations.

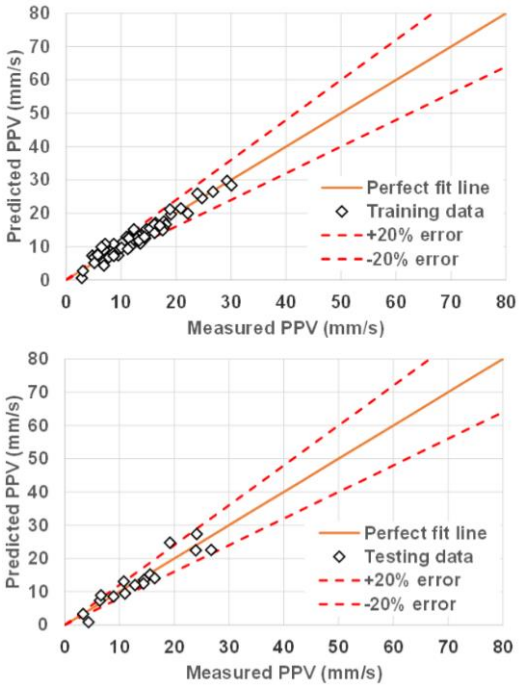

Fig. 4 Relationship between measured and predicted PPV achieved using the GEP model

9. Development of the MOGA-EPR model

The same training and testing datasets which used in the development of the GEP model have also been used in the development of the MOGA-EPR model to ensure consistency and to allow fair comparison of the accuracy of both models (MOGA-EPR and GEP models).

In addition, many trails have been undertaken to examine the effect of the model exponents, number of terms and model structure. This has been conducted by changing the number of terms of the developed model (i.e., two terms, three terms, four terms…etc.), the range of the exponents of the developed model and the general form of the mathematical relationship between the dependent and independent variables. The statistical performance of the developed model has been thorough checked with each change of any of the aforementioned parameters (model exponents, number of terms, and model structure) by calculating the MAE, $RMSE$, μ, σ, $a20-index$, and R^2. The best MOGA-EPR model obtained from the trials is shown in Eq. (19).

Table 8 Equations extracted from the GEP model to prediction of the PPV

Model	Formula
GEP	$PPV = [\frac{(W\times G_1C_4)+(Vp+D)}{G_1C_9\times G_1C_2+D} - Vp] + [(Vp - (\frac{Vp}{(G_2C_8\times G_2C_9-D)\times(G_2C_1+\mathrm{SL})})] + [\frac{\mathrm{SL}.Vp}{(G_3C_0\times D-G_3C_5)-(SL\times G_3C_1)}]$;
Coefficients	G_1C_4 = 10.6938151473838; G_1C_9 = 7.6750589102085; G_1C_2 = 6.84825564513972; G_2C_1 = 1.45337286754221; G_2C_8 = 160.150151820157; G_2C_9 = 3.05345057670047; G_3C_5 = -40.7329830170773; G_3C_1 = 43.834285177175; G_3C_0 = -7.77898269233453

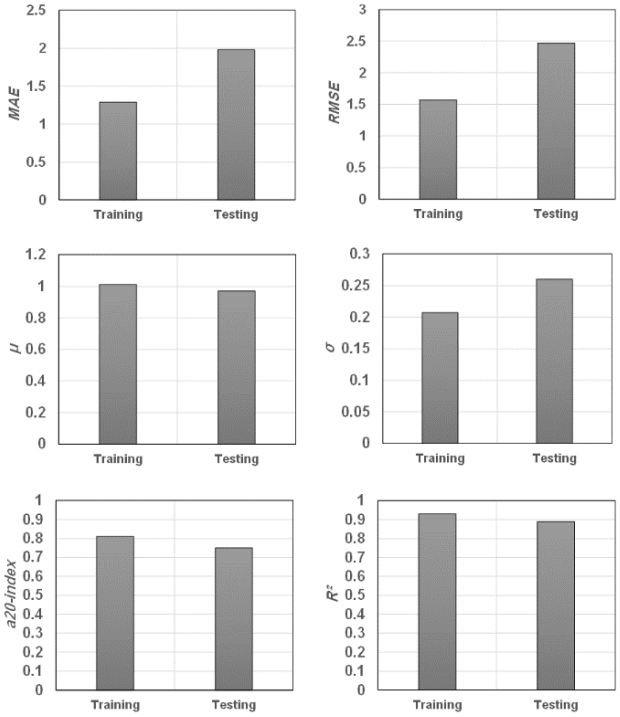

Fig. 5 Statistical performance indicators of the training and testing data for the GEP model

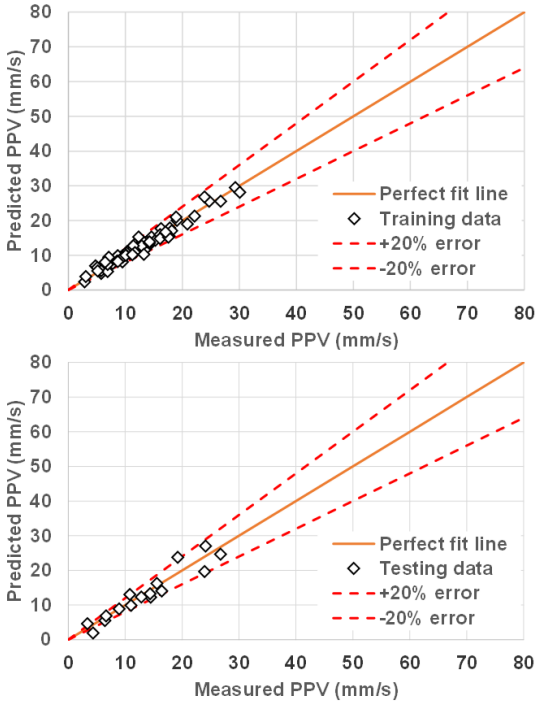

Fig. 6 Relationship between measured and predicted PPV using the MOGA-EPR

$$PPV = -20.91 \times \sqrt{D} + 0.92 \times D - 0.0006 \times D^2 + 1.15 \times \sqrt{W} - 0.5 \times 10^{-9} \times D^2 \times W \times \sqrt{SL} \times \sqrt{Vp} + 133.23 \quad (19)$$

Fig. 6 presents the predicted-measured relationship for the training and testing data, respectively. It is quite obvious from both figures that most of the predictions are very close to the perfect fit line. Furthermore, most of the predictions are also within the ±20% error indicating excellent predictions.

To provide more insight into the performance of the proposed model, Fig. 7 presents the results of the statistical performance indicators (MAE, $RMSE$, μ, σ, $a20-index$, and R^2) for the training and testing data. The figure clearly show that the proposed model predicts the PPV with low mean absolute error (0.96 for training data and 1.81 for testing data) and low root mean square error (1.24 for training data and 2.22 for testing data). In addition, the results of the mean and the standard deviation of the predicted to measured values also confirm the quality of the proposed model, where the obtained mean is approximately equal to 1.0 for both training and testing data and also the standard deviation of the measured to predicted results is very close to zero for both training and testing data. Furthermore, the results of the $a20-index$ show that the proposed model predicts 87% of the training data and 75% of the testing data within error equal to or less than 20%, indicating again excellent accuracy of predictions. Finally, the results of the coefficient of determination confirm the observations noted from the figure of the relationship between measured and predicted data (Fig. 6), where the proposed model achieved R^2 of 0.96 for the training data and 0.91 for the testing data, indicating again excellent predictions.

Comparing the statistical performance of the proposed model (Fig. 7) with the performance of the equations currently available (Tables 5 and 6) and the performance of the GEP (Fig. 5) shows that the proposed model is superior as the it scored much better statistical performance indicators compared to the available equations and the GEP model. This also provides additional support to the quality of the new model. Thus, the proposed model is recommended for much better accuracy in the design and analysis.

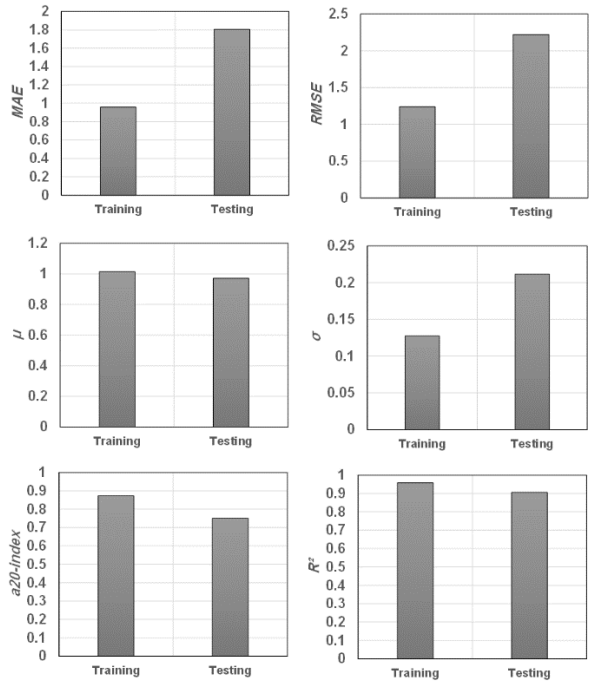

Fig. 7 Statistical performance indicators of the training and testing data for the MOGA-EPR model

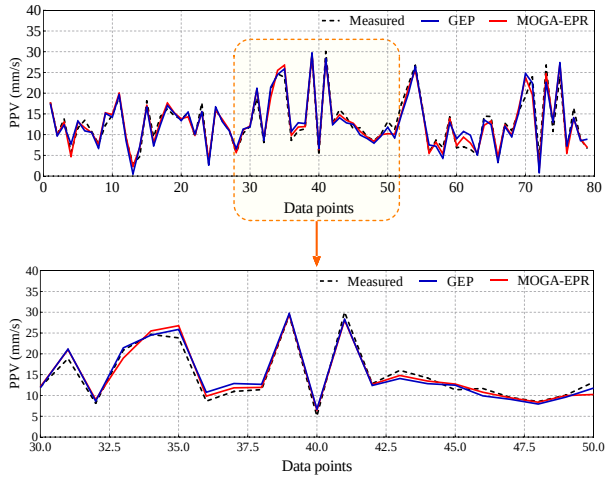

Fig. 8 The performance evaluation of MOGA-EPR and GEP models versus the measured *PPV* values

10. Discussions

The discussions of this paper include three parts, i.e., compatibility assessment of the models, error analysis and sensitivity analysis.

10.1 Compatibility assessment of the models

Assessing the compatibility of machine learning based models with observational values is one of the most important steps in the validation. Fig. 8 depicts the physical expected trend of *PPV* prediction using the MOGA-EPR and GEP models. Variation trend of the *PPV* demonstrates that the data driven models perform successfully in capturing the non-linear behavior of measured *PPV* results.

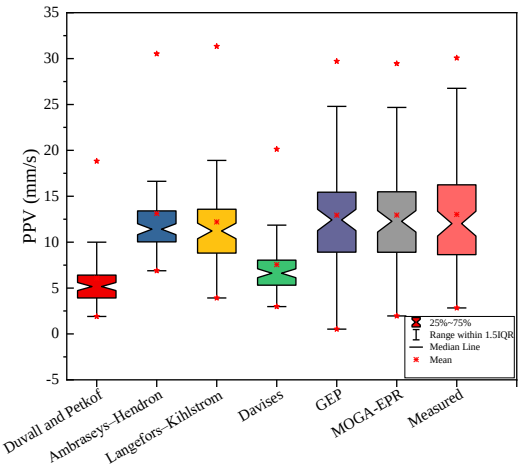

Percentiles/ Metrics	Empirical based models			Data-driven			Measured
	Duvall and Petkof	Ambraseys –Hendron	Langefors– Kihlstrom	Davises	GEP	MOGA -EPR	
Q_{25}%	3.925	10.03	8.81	5.314	8.91	8.903	8.64
Q_{50}%	5.168	11.41	11.22	6.615	12.42	12.27	12.02
Q_{75}%	6.404	13.4	13.58	8.035	15.44	15.48	16.25
IQR	2.479	3.37	4.77	2.721	6.53	6.58	7.61
Std. Deviation	3.498	5.424	5.399	3.621	6.251	6.212	6.263

Fig. 9 Distribution function comparison between measured and predicted *PPV* values using data-driven and empirical equations

However, magnifying the trend plot confirmed the MOGA-EPR provides more promising accuracy than the GEP approach.

In order to quantify the uncertainty assessment of the predictive models, the notched box of predicted (data driven and empirical equations) and measured values of *PPV* are shown in Fig. 9. According to the presented distribution functions, it can be found that the MOGA-EPR and GEP models have more appropriated consistency with the measured values than the empirical equations. Moreover, the percentiles values (Q_{25}%, Q_{50}%, and Q_{75}%) and interquartile range (IQR: Q_{75}%-Q_{25}%) were examined to scrutinize the performance assessment of the models under study (Jamei *et al.* 2021). The MOGA-EPR model on account of having the closest IQR (6.58) to the observed values (7.61) were identified as the best predictive model followed by the GEP model (6.53), and Langefors-Kihlstrom equation (4.77). In addition, the Langefors-Kihlstrom equation have the most promising outcomes among all the considered empirical equations.

10.2 Error analysis

In the next stage of the model's validation, two type of error analysis including the relative deviation ($RD = 100 \times (PPV_{Measured} - PPV_{predicted})/PPV_{Measured}$) and cumulative frequency of absolute percentage of relative deviation were adopted to evaluate the accuracy and efficiency of the provided models (Jamei *et al* 2021). Fig. 10 demonstrates the relative deviation distribution function using A notched box plot for both training (Left Panel) and testing (Right panel) of data driven models. According to Fig. 10, the interquartile (IQR) domain of the MOGA-EPR

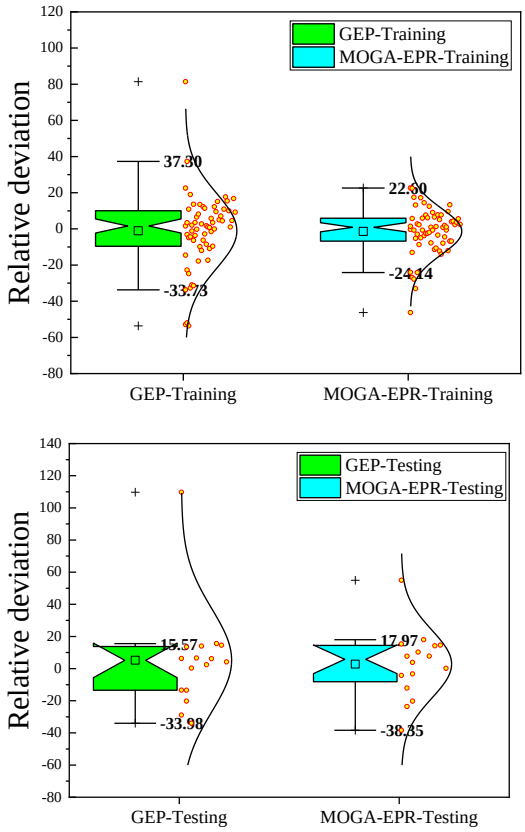

Fig. 10 The relative deviation (%) distribution for training (Left) and testing (Right) datasets

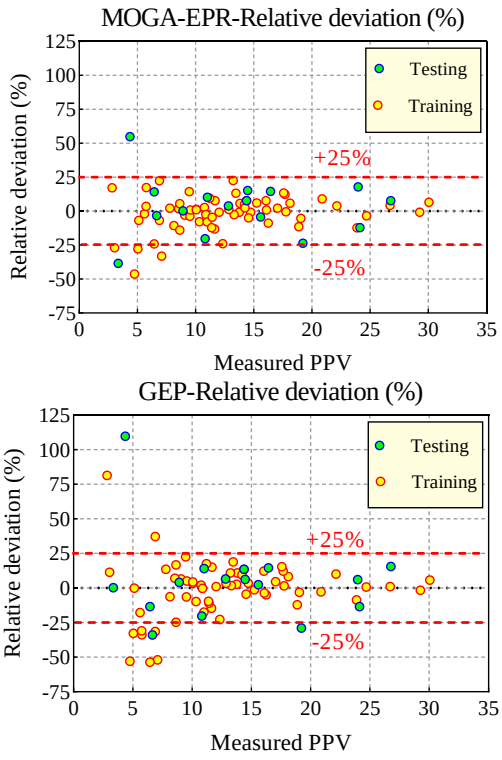

Fig. 11 The relative deviation scattered distribution of the MOGA-EPR and GEP approaches for both training and testing phases

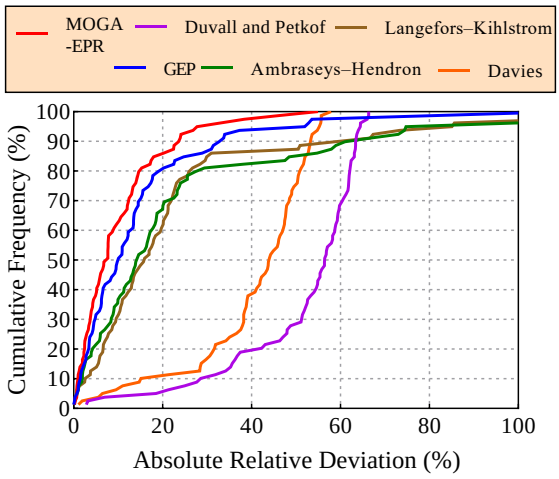

Fig. 12 The cumulative frequency versus absolute percentage of the relative deviation for outcome of data-driven models and empirical equations

model (46.74%) in training dataset is lower than GEP model (71.03%) whereas in testing data set the IQR domain of the GEP model (49.55%) is lower than that of the MOGA-EPR model (56.14%). However, the distribution probability function of the MOGA-EPR model is more compacted than the GEP model and leads to less relative deviations.

Fig. 11 demonstrates the scattered plots of relative deviation of provided data driven methods. It is crystal clear that the MOGA-EPR model by lower range of ($-46.26 \leq RD \leq 54.95\%$) yields more reliable results than the GEP model ($-53.6 \leq RD \leq 109.7\%$). As can be seen, the exceeding points of relative deviation in both training and testing datasets in the GEP model are higher than those of the MOGA-EPR approach. The aforementioned error analysis inferred that the MOGA-EPR is superior to the GEP in predicting the *PPV* values.

To specifying the capability of data driven models versus the existing empirical equations, the cumulative frequency of the absolute percentage of the relative deviation were reported in Fig. 12. This figure shows that more than 80% of the predicted datasets yield less than absolute relative deviation about 14.65%, whereas the GEP model, and Langeofors-Kihlstrom, Ambraseys-Hendron, Davies, and Duvall and Petkof equations provided absolute relative deviation about 18.98%, 22.14%, 22.5%, 48.55%, and 60.77%, respectively. Thus, it can be inferred that the MOGA-EPR has the best predictive performance than the GEP model and the available equations. In addition, the GEP model scored second compared to the other empirical equations. Notably, it is worthy to state that the developed MOGA-EPR and GEP models scored better than the other empirical equations because the developed models utilized more than one influential parameter and thus, provided more accurate predictions, while the empirical equations only utilized one of the important influential parameters.

6.3 Sensitivity analysis

To investigate the effect of input variables on the output

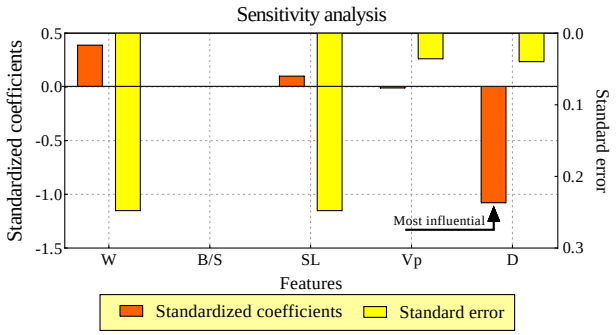

Fig. 13 The sensitivity analysis outcome in terms of standardized coefficient and standard error

of the model, a regression analysis was performed. For this purpose, the standardized coefficient was computed as the most important component of regression analysis on all data to determine the effect of each input variable (independent variable) on the target output (dependent variable). The standardized coefficient relationship is as follows (Rehamina *et al.* 2021)

$$Sc^* = Sc\frac{St.D_x}{St.D_y} \quad (20)$$

In the above relation, Sc is the linear regression coefficients fitted to the data, $St.D_x$ and $St.D_y$ are the standard deviations of the input and target data, respectively. The higher value of the standardized coefficient shows the higher effect of the variable on the model output. According to the Table 9 and Figure 13, the highest value of the standardized coefficient is related to the input variable of D ($Sc = -1.08$). The W ($Sc = 0.931$) and SL ($Sc = 0.103$) variables are the second and third parameters affecting the output of the model, respectively. D and Vp have the minimum values of standard error (0.04 and 0.036, respectively). However, the standardized coefficient is the critical metric on sensitivity analysis. Besides, the zero values in the regression analysis of parameter B/S indicate that this factor has been omitted due to the small effect of the regression analysis.

11. Conclusions

Ground vibration is considered as one of the most important undesirable effects of blast operations which needs to be precisely predicted to minimize the potential risk of damage. Although some empirical equations have been presented to predict ground vibration empirically, the performance of these equations still needs to be improved. Furthermore, these empirical equations have been developed based on considering only two of the influential parameters on ground vibration, and this subject is one of disadvantages of empirical equations. For solving this problem, the present study proposed an efficient and accurate mathematical model to predict ground vibration by utilizing the MOGA-EPR. The new model uses five influential parameters and thus, provide much better accuracy of prediction compared with the available empirical equations. Furthermore, a GEP model has also been developed as part of the study to check the performance of the MOGA-EPR. The data collected from the studied case (Harapan Ramai quarry) has been utilized in the development of the MOGA-EPR and GEP models, and also in the accuracy checks. For a fair compression, statistical error indicators (i.e., MAE, $RMSE$, μ, σ, R^2 and $a20-index$) have been utilized in the accuracy check. The findings and conclusions of this study can be briefly listed as follows:

Table 9 The sensitivity analysis results using a regression analysis

Source	S. Cof.	Standard error	t	$Pr>\|t\|$	Lower bound (95%)	Upper bound (95%)
W	0.39	0.25	1.58	0.12	-0.10	0.88
B/S	0.00	0.00	0.00	0.00	0.00	0.00
SL	0.10	0.25	0.42	0.68	-0.39	0.60
Vp	-0.01	0.04	-0.32	0.75	-0.08	0.06
D	-1.08	0.04	-26.75	<0.0001	-1.16	-0.99

- The most optimal values of MAE, $RMSE$, μ, σ, R^2 and $a20-index$ indicators were obtained from the MOGA-EPR model. This clearly indicates the effectiveness of the MOGA-EPR model in predicting the ground vibration. The GEP model and empirical equations were identified as the next categories, respectively. Among the empirical equations, the Ambraseys-Hendron and Duvall and Petkof were the best and worst equations, respectively, in terms of prediction accuracy.
- A standardized coefficient analysis was performed as the sensitivity analysis, and according to its results, the D was identified as the most influential parameter upon PPV.
- In the present study, an explicit model has been mined using the MOGA-EPR which is not possible in black box soft computing methods (such as the ANN). The extracted model can be used in future to optimize designs or to compare the performance of the MOGA-EPR against other soft computing methods.
- Furthermore, the ability of the MOGA-EPR model can be enhanced by using other objectives within the EPR framework to enable better selection of the optimum model within the searching iterations.

References

Abbas, A.S. and Asheghi, R. (2018), "Optimized developed artificial neural network-based models to predict the blast-induced ground vibration", *Innov. Infrastr. Solut.*, **3**, 1-10. https://doi.org/10.1007/s41062-018-0137-4,

Alkroosh, I., Alzabeebee, S. and Al-Taie, A.J. (2020), "Evaluation of the accuracy of commonly used empirical correlations in predicting the compression index of Iraqi fine-grained soils", *Innov. Infrastr. Solut.*, **5**, 68. https://doi.org/10.1007/s41062-020-00321-y.

Alzabeebee, S. (2019), "Seismic response and design of buried concrete pipes subjected to soil loads", *Tunn. Undergr. Sp. Technol.*, **93**, 103084. https://doi.org/10.1016/j.tust.2019.103084.

Alzabeebee, S. (2020), "Dynamic response and design of a skirted

strip foundation subjected to vertical vibration", *Geomech. Eng.*, **20**(4), 345-358. https://doi.org/10.12989/gae.2020.20.4.345.

Alzabeebee, S. (2022a), "Application of EPR-MOGA in computing the liquefaction-induced settlement of a building subjected to seismic shake", *Eng. Comput.*, **38**, 437-448. https://doi.org/10.1007/s00366-020-01159-9.

Alzabeebee, S. (2022b), "Explicit soft computing model to predict the undrained bearing capacity of footing resting on aggregate pier reinforced cohesive ground", *Innov. Infrastr. Solut.*, **7**, 105. https://doi.org/10.1007/s41062-021-00706-7.

Alzabeebee, S. and Chapman, D.N. (2020), "Evolutionary computing to determine the skin friction capacity of piles embedded in clay and evaluation of the available analytical methods", *Transp. Geotechnol.*, **24**, 100372. https://doi.org/10.1016/j.trgeo.2020.100372.

Alzabeebee, S., Mohammed, D.A. and Alshkane, Y.M. (2022b), "Experimental study and soft computing modeling of the unconfined compressive strength of limestone rocks considering dry and saturation conditions", *Rock Mech. Rock Eng.*, **55**, 5535-5554. https://doi.org/10.1007/s00603-022-02948-y.

Alzabeebee, S., Zuhaira, A.A. and Al-Hamd, R.K.S. (2022a), "Development of an optimized model to compute the undrained shaft friction adhesion factor of bored piles", *Geomech. Eng.*, **28**(4), 397-404. https://doi.org/10.12989/gae.2022.28.4.397.

Ambraseys, N.R. and Hendron, A.J. (1968), *Dynamic Behaviour of Rock Masses Rock Mechanics in Engineering Practices*, Wiley, London.

Armaghani, D.J., Mamou, A., Maraveas, C., Roussis, P.C., Siorikis, V.G., Skentou, A.D. and Asteris, P.G. (2021), "Predicting the unconfined compressive strength of granite using only two non-destructive test indexes", *Geomech. Eng.*, **25**(4), 317-330. https://doi.org/10.12989/gae.2021.25.4.317.

Armaghani, J., Kumar, D., Samui, D., Hasanipanah, M. and Roy, B. (2020), "A novel approach for forecasting of ground vibrations resulting from blasting: modified particle swarm optimization coupled extreme learning machine", *Eng. Comput.*, **37**(4), 3221-3235. https://doi.org/10.1007/s00366-020-00997-x.

Arthur, C.K., Temeng, V.A. and Ziggah, Y.Y. (2020), "Multivariate Adaptive Regression Splines (MARS) approach to blast-induced ground vibration prediction", *Int. J. Min. Reclam. Environ.*, **34**(3), 198-222. https://doi.org/10.1080/17480930.2019.1577940.

Aytek, A. and Kişi, Ö. (2008), "A genetic programming approach to suspended sediment modelling", *J. Hydro.*, **351**(3), 288-298. https://doi.org/10.1016/j.jhydrol.2007.12.005.

Bai, X.D., Cheng, W.C., Ong, D.E. and Li, G. (2021), "Evaluation of geological conditions and clogging of tunneling using machine learning", *Geomech. Eng.*, **25**(1), 59-73. https://doi.org/10.12989/gae.2021.25.1.059.

Bui, X., Choi, Y., Atrushkevich, V., Nguyen, H., Tran, Q.H., Long, N.Q. and Hoang, H.T. (2020), "Prediction of blast-induced ground vibration intensity in open-pit mines using unmanned aerial vehicle and a novel intelligence system", *Nat. Resour. Res.,* **29**, 771-790. https://doi.org/10.1007/s11053-019-09573-7.

Bui, X.N., Nguyen, H., Tran, Q.H., Nguyen, D.A. and Bui, H.B. (2021), "Predicting ground vibrations due to mine blasting using a novel artificial neural network-based cuckoo search optimization", *Nat. Resour. Res.*, **30**(3), 2663-2685. https://doi.org/10.1007/s11053-021-09823-7.

Chen, W., Hasanipanah, M., Rad, H.N., Armaghani, D.J. and Tahir, M.M. (2021), "A new design of evolutionary hybrid optimization of SVR model in predicting the blast-induced ground vibration", *Eng. Comput.*, **37**, 1455-1471. https://doi.org/10.1007/s00366-019-00895-x.

Davies, B., Farmer, I.W. and Attewell, P.B. (1964), "Ground vibrations from shallow sub-surface blasts", *Eng.*, **217**, 553-559.

Ding, Z., Nguyen, H., Bui, X., Zhou, J. and Moayedi, H. (2019), "Computational intelligence model for estimating intensity of blast-induced ground vibration in a mine based on imperialist competitive and extreme gradient boosting algorithms", *Nat. Resour. Res.*, **29**(2), 751-769. https://doi.org/10.1007/s11053-019-09548-8.

Duvall, W.I. and Petkof, B.B. (1959), "Spherical propagation of explosion generated strain pulses in rock", US Bur Mines, RI 5483.

Fang, Q., Nguyen, H., Bui, X.N. and Nguyen-Thoi, T. (2019a), "Prediction of blast-induced ground vibration in open-pit mines using a new technique based on imperialist competitive algorithm and M5Rules", *Nat. Resour. Res.*, **29**(2), 791-806. https://doi.org/10.1007/s11053-019-09577-3.

Faradonbeh, R.S., Armaghani, D.J., Abd Majid, M.Z., Tahir, M. M.D., Murlidhar, B.R., Monjezi, M. and Wong, H.M. (2016), "Prediction of ground vibration due to quarry blasting based on gene expression programming: A new model for peak particle velocity prediction", *Int. J. Environ. Sci. Technol.*, **13**(6), 1453-1464. https://doi.org/10.1007/s13762-016-0979-2.

Fattahi, H. and Hasanipanah, M. (2021), "Prediction of blast-induced ground vibration in a mine using relevance vector regression optimized by metaheuristic algorithms", *Nat. Resour. Res.*, **30**(2), 1849-1863. https://doi.org/10.1007/s11053-020-09764-7.

Ferreira, C. (2001), "Gene expression programming: A new adaptive algorithm for solving problems", arXiv preprint cs/0102027.

Ferreira, C. (2002), "Gene expression programming in problem solving", *Soft Computing and Industry*, Springer, London..

Gandomi, A.H., Alavi, A.H. and Ryan, C. (2015), *Handbook of Genetic Programming Applications*, Springer.

Ghasemi, E., Ataei, M. and Hashemolhosseini, H. (2013), "Development of a fuzzy model for predicting ground vibration caused by rock blasting in surface mining", *J. Vib. Control*, **19**(5), 755-770. https://doi.org/10.1177/1077546312437002.

Gholampour, A., Gandomi, A.H. and Ozbakkaloglu, T. (2017), "New formulations for mechanical properties of recycled aggregate concrete using gene expression programming", *Constr. Build. Mater.*, **130**, 122-145. https://doi.org/10.1016/j.conbuildmat.2016.10.114.

Giustolisi, O. and Savic, D.A. (2006), "A symbolic data-driven technique based on evolutionary polynomial regression", *J. Hydroinform*, **8**(3), 207-222. http://doi.org/10.2166/hydro.2006.020.

Giustolisi, O. and Savic, D.A. (2009), "Advances in data-driven analyses and modelling using EPR-MOGA", *J. Hydroinform.*, **11**(3-4), 225-236. https://doi.org/10.2166/hydro.2009.017.

Hajihassani, M., Armaghani, D.J., Monjezi, M., Mohamad, E.T. and Marto, A. (2015), "Blast-induced air and ground vibration prediction: A particle swarm optimization-based artificial neural network approach", *Environ. Earth Sci.*, **74**(4), 2799-2817. https://doi.org/10.1007/s12665-015-4274-1.

Hasanipanah, M. and Amnieh, H.B. (2020a), "A fuzzy rule-based approach to address uncertainty in risk assessment and prediction of blast-induced Flyrock in a quarry", *Nat. Resour. Res.*, **29**(2), 669-689. https://doi.org/10.1007/s11053-020-09616-4.

Hasanipanah, M. and Amnieh, H.B. (2020b), "Developing a new uncertain rule-based fuzzy approach for evaluating the blast-induced backbreak", *Eng. Comput.*, **37**(3), 1879-1893. https://doi.org/10.1007/s00366-019-00919-6.

Hasanipanah, M., Faradonbeh, R.S., Amnieh, H.B., Armaghani, D.J. and Monjezi, M. (2017), "Forecasting blast-induced ground vibration developing a CART model", *Eng. Comput.*, **33**(2), 307-316. https://doi.org/10.1007/s00366-016-0475-9.

Hasanipanah, M., Keshtegar, B., Thai, D.K. and Troung, N.T. (2020a), "An ANN adaptive dynamical harmony search algorithm to approximate the flyrock resulting from blasting", *Eng. Comput.*, 1-13. https://doi.org/10.1007/s00366-020-01105-9.

Hasanipanah, M., Monjezi, M., Shahnazar, A., Armaghani, D.J. and Farazmand, A. (2015), "Feasibility of indirect determination of blast induced ground vibration based on support vector machine", *Measure.*, **75**, 289-297. https://doi.org/10.1016/j.measurement.2015.07.019.

Hasanipanah, M., Zhang, W., Armaghani, D.J. and Rad, H.N. (2020b), "The potential application of a new intelligent based approach in predicting the tensile strength of rock", *IEEE Access*, **8**, 57148-57157. https://doi.org/10.1109/access.2020.2980623.

Huang, J., Duan, T., Zhang, Y., Liu, J., Zhang, J. and Lei, Y. (2020), "Predicting the permeability of pervious concrete based on the beetle antennae search algorithm and random forest model", *Adv. Civil Eng.*, **2020**, Article ID 8863181. https://doi.org/10.1155/2020/8863181.

Huang, J., Sun, Y. and Zhang, J. (2021), "Reduction of computational error by optimizing SVR kernel coefficients to simulate concrete compressive strength through the use of a human learning optimization algorithm", *Eng. Comput.*, **38**(4), 3151-3168. https://doi.org/10.1007/s00366-021-01305-x.

Jamei, M., Karbasi, M., Olumegbon, I.A., Moshraf-Dehkordi, M., Ahmadianfar, I. and Asadi, A. (2021), "Specific heat capacity of molten salt-based nanofluid in solar thermal applications: A paradigm of two modern ensemble machine learning methods", *J. Molecul. Liquid.*, **335**, 116434. https://doi.org/10.1016/j.molliq.2021.116434.

Jelušič, P., Ivanič, A. and Lubej, S. (2021), "Prediction of blast-induced ground vibration using an adaptive network-based fuzzy inference system", *Appl. Sci.*, **11**(1), 203. https://doi.org/10.3390/app11010203.

Kamran, M., Shahani, N.M. and Armaghani, D.J. (2022), "Decision support system for underground coal pillar stability using unsupervised and supervised machine learning approaches", *Geomech. Eng.*, **30**(2), 107-121. https://doi.org/10.12989/gae.2022.30.2.107.

Khandelwal, M., Kumar, D.L. and Yellishetty, M. (2011), "Application of soft computing to predict blast-induced ground vibration", *Eng. Comput.*, **27**(2), 117-125. https://doi.org/10.1007/s00366-009-0157-y.

Koopialipoor, M., Fallah, A., Armaghani, D.J., Azizi, A. and Mohamad, E.T. (2019), "Three hybrid intelligent models in estimating flyrock distance resulting from blasting", *Eng. Comput.*, **35**, 243-256. https://doi.org/10.1007/s00366-018-0596-4.

Koza, J.R. (1992), *Genetic Programming: On the Programming of Computers by Means of Natural Selection*, MIT Press, Cambridge, MA.

Kwak, N.S. and Ko, T.Y. (2022), "Machine learning-based regression analysis for estimating Cerchar abrasivity index", *Geomech. Eng.*, **29**(3), 219-228. https://doi.org/10.12989/gae.2022.29.3.219.

Langefors, U. and Kihlstrom, B. (1963), *The Modern Technique of Rock Blasting*, Wiley, New York.

Lawal, A.I., Kwon, S. and Kim, G.Y. (2021b), "Prediction of the blast-induced ground vibration in tunnel blasting using ANN, moth-flame optimized ANN, and gene expression programming", *Acta Geophys.*, **69**, 161-174. https://doi.org/10.1007/s11600-020-00532-y.

Lawal, A.I., Kwon, S., Hammed, O.S. and Idris, M.A. (2021a), "Blast-induced ground vibration prediction in granite quarries: An application of gene expression programming, ANFIS, and sine cosine algorithm optimized ANN", *Int. J. Min. Sci. Technol.*, **31**(2), 265-277. https://doi.org/10.1016/j.ijmst.2021.01.007.

Luat, N.V., Lee, K. and Thai, D.K. (2020a), "Application of artificial neural networks in settlement prediction of shallow foundations on sandy soils", *Geomech. Eng.*, **20**(5), 385-397. https://doi.org/10.12989/gae.2020.20.5.385.

Luat, N.V., Nguyen, V.Q., Lee, S., Woo, S. and Lee, K. (2020b), "An evolutionary hybrid optimization of MARS model in predicting settlement of shallow foundations on sandy soils", *Geomech. Eng.*, **21**(6), 583-598. https://doi.org/10.12989/gae.2020.21.6.583.

Monjezi, M., Hasanipanah, M. and Khandelwal, M. (2013), "Evaluation and prediction of blast-induced ground vibration at Shur River Dam, Iran, by artificial neural network", *Neur. Comput. Appl.*, **22**(7-8), 1637-1643. https://doi.org/10.1007/s00521-012-0856-y.

Nguyen, H., Bui, X.N., Tran, Q.H., Nguyen, H.A., Nguyen, D.A. and Le, Q.T. (2021), "Prediction of ground vibration intensity in mine blasting using the novel hybrid MARS-PSO-MLP model", *Eng. Comput.*, 1-19. https://doi.org/10.1007/s00366-021-01332-8.

Nguyen, H., Choi, Y., Bui, X.N. and Nguyen-Thoi, T. (2020b), "Predicting blast-induced ground vibration in open-pit mines using vibration sensors and support vector regression-based optimization algorithms", *Sensor.*, **20**(1), 132. https://doi.org/10.3390/s20010132.

Nguyen, H., Drebenstedt, C., Bui, X.N. and Bui, D.T. (2020a), "Prediction of blast-induced ground vibration in an open-pit mine by a novel hybrid model based on clustering and artificial neural network", *Nat. Resour. Res.*, **29**, 691-709. https://doi.org/10.1007/s11053-019-09470-z.

Rajabi, A.M. and Vafaee, A. (2020), Prediction of blast-induced ground vibration using empirical models and artificial neural network (Bakhtiari Dam access tunnel, as a case study)", *J. Vib. Control*, **26**(7-8), 520-531. https://doi.org/10.1177/1077546319889844.

Rehamnia, I., Benlaoukli, B., Jamei, M., Karbasi, M. and Anurag M. (2021), "Simulation of seepage flow through embankment dam by using a novel extended kalman filter based neural network paradigm: case study of fontaine Gazelles Dam, Algeria", *Measure.*, **176**, 109219. https://doi.org/10.1016/j.measurement.2021.109219.

Saadat, M., Khandelwal, M. and Monjezi, M. (2014), "An ANN-based approach to predict blast-induced ground vibration of Gol-E-Gohar iron ore mine, Iran", *J. Rock Mech. Geotech. Eng.*, **6**(1), 67-76. https://doi.org/10.1016/j.jrmge.2013.11.001.

Sasmal, S.K. and Behera, R.N. (2021), "Application of artificial intelligence methods for predicting transient response of foundation", *Geomech. Eng.*, **27**(3), 197-211. https://doi.org/10.12989/gae.2021.27.3.197.

Shams, M.A., Shahin, M.A. and Ismail, M.A. (2020), "Design of stiffened slab foundations on reactive soils using 3D numerical modeling", *Int. J. Geomech.*, **20**(7), 04020097. https://doi.org/10.1061/(ASCE)GM.1943-5622.0001654.

Wang, H.L., Yin, Z.Y., Zhang, P. and Jin, Y.F. (2020), "Straightforward prediction for air-entry value of compacted soils using machine learning algorithms", *Eng. Geol.*, **279**, 105911. https://doi.org/10.1016/j.enggeo.2020.105911.

Yu, Z., Shi, X., Zhou, J., Chen, X. and Qiu, X. (2020), "Effective assessment of blast-induced ground vibration using an optimized random forest model based on a Harris hawks optimization algorithm", *Appl. Sci.*, **10**(4), 1403. https://doi.org/10.3390/app10041403.

Zhang W., Zhang Y., Gu X., Wu C., Han L. (2022), "Prediction for TBM penetration rate using four hyperparameter optimization methods and RF model", *Application of Soft Computing, Machine Learning, Deep Learning and Optimizations in Geoengineering and Geoscience*, Springer, Singapore.

Zhang, J., Sun, Y., Li, G., Wang, Y., Sun, J. and Li, J. (2020), "Machine-learning-assisted shear strength prediction of reinforced concrete beams with and without stirrups", *Eng. Comput.*, 1-15. https://doi.org/10.1007/s00366-020-01076-x.

Zhang, W., Li, H., Li, Y., Liu, H., Chen, Y. and Ding, X. (2021a), "Application of deep learning algorithms in geotechnical

engineering: A short critical review", *Artif. Intel. Rev.*, **54**, 5633-5673. https://doi.org/10.1007/s10462-021-09967-1.

Zhang, X., Nguyen, H., Bui, X.N., Tran, Q.H., Nguyen, D.A., Tien Bui, D. and Moayedi, H. (2019), "Novel soft computing model for predicting blast-induced ground vibration in open-pit mines based on particle swarm optimization and XGBoost", *Nat. Resour. Res.*, **29**(2), 711-721. https://doi.org/10.1007/s11053-019-09492-7.

Zhang, Y., Wen, H., Xie, P., Hu, D., Zhang, J. and Zhang, W. (2021b), "Hybrid-optimized logistic regression model of landslide susceptibility along mountain highway", *Bull. Eng. Geol. Environ*., **80**(10), 7385-7401. https://doi.org/10.1007/s10064-021-02415-y.

Zhou, J., Asteris, P.G., Armaghani, D.J. and Pham, B.T. (2020), "Prediction of ground vibration induced by blasting operations through the use of the Bayesian Network and random forest models", *Soil Dyn. Earthq. Eng*., **139**, 106390. https://doi.org/10.1016/j.soildyn.2020.106390.

Zhou, J., Li, E., Yang, S., Wang, M., Shi, X., Yao, S. and Mitri, H.S. (2019) "Slope stability prediction for circular mode failure using gradient boosting machine approach based on an updated database of case histories", *Saf. Sci*., **118**, 505-518. https://doi.org/10.1016/j.ssci.2019.05.046.

Zhou, J., Li, X. and Mitri, H.S. (2015), "Comparative performance of six supervised learning methods for the development of models of hard rock pillar stability prediction", *Nat. Hazard.*, **79**, 291-316. https://doi.org/10.1007/s11069-015-1842-3.

Zhou, J., Shi, X. and Li, X. (2016), "Utilizing gradient boosted machine for the prediction of damage to residential structures owing to blasting vibrations of open pit mining", *J. Vib. Control*, **22**(19), 3986-3997. https://doi.org/10.1177/1077546314568172.

Zhou, J., Shi, X., Du, K., Qiu, X., Li, X. and Mitri, H.S. (2017), "Feasibility of random-forest approach for prediction of ground settlements induced by the construction of a shield-driven tunnel", *Int. J. Geomech*., **17**(6), 04016129. https://doi.org/10.1061/(ASCE)GM.1943-5622.0000817.

Zhu, W., Rad, H.N. and Hasanipanah, M. (2021), "A chaos recurrent ANFIS optimized by PSO to predict ground vibration generated in rock blasting", *Appl. Soft Comput.*, **108**, 107434. https://doi.org/10.1016/j.asoc.2021.107434.

Zuhaira, A.A., Al-Hamd, R.K.S., Alzabeebee, S. and Cunningham, L.S. (2021), "Numerical investigation of skimming flow characteristics over non-uniform gabion-stepped spillways", *Innov. Infrastr. Solut*., **6**, 225. https://doi.org/10.1007/s41062-021-00579-w.